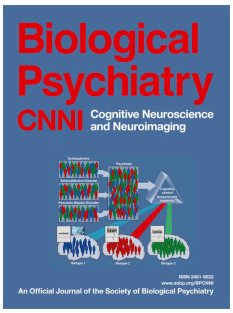

Dynamic Functional Hyperconnectivity after Psilocybin Intake is Primarily Associated with Oceanic Boundlessness

Sepehr Mortaheb, Larry D. Fort, Natasha L. Mason, Pablo Mallaroni, Johannes G. Ramaekers, Athena Demertzi

PII: S2451-9022(24)00084-3

DOI: https://doi.org/10.1016/j.bpsc.2024.04.001

Reference: BPSC 1203

To appear in: *Biological Psychiatry: Cognitive Neuroscience and Neuroimaging*

Received Date: 20 January 2024

Revised Date: 28 March 2024

Accepted Date: 1 April 2024

Please cite this article as: Mortaheb S., Fort L.D., Mason N.L., Mallaroni P., Ramaekers J.G. & Demertzi A., Dynamic Functional Hyperconnectivity after Psilocybin Intake is Primarily Associated with Oceanic Boundlessness, *Biological Psychiatry: Cognitive Neuroscience and Neuroimaging* (2024), doi: https://doi.org/10.1016/j.bpsc.2024.04.001.

Type: Archival Reports

Running Title: Dynamic Functional Hyperconnectivity after Psilocybin

Dynamic Functional Hyperconnectivity after Psilocybin Intake is Primarily Associated with Oceanic Boundlessness

Sepehr Mortaheb[1,2±], Larry D. Fort[1,2±], Natasha L. Mason[3], Pablo Mallaroni[3], Johannes G. Ramaekers[3*±], Athena Demertzi[1,2,4*±]

[1]Physiology of Cognition, GIGA-CRC In Vivo Imaging, University of Liège, Belgium
[2]Fund for Scientific Research FNRS, Brussels, Belgium
[3]Department of Neuropsychology and Psychopharmacology, Faculty of Psychology and Neuroscience, Maastricht University, The Netherlands
[4]Psychology & Neuroscience of Cognition (PsyNCog), University of Liège, Belgium

[±]Equal contribution

[*]Corresponding authors:
a.demertzi@uliege.be
j.ramaekers@maastrichtuniversity.nl

Keywords: psilocybin, connectivity, dynamics, fMRI, 5D-ASC, global signal

Abstract

Background: Psilocybin is a widely studied psychedelic substance, which leads to the psychedelic state, a specific altered state of consciousness. To date, the relationship between the psychedelic state's neurobiological and experiential patterns remains under-characterized as they are often analyzed separately. We investigated the relationship between neurobiological and experiential patterns after psilocybin by focusing on the link between dynamic cerebral connectivity and retrospective questionnaire assessment. **Methods**: Healthy participants were randomized to receive either psilocybin (n=22) or placebo (n=27) and scanned for six minutes in eyes open resting state during the peak subjective drug effect (102 minutes post-treatment) in ultra-high field 7T MRI. The 5D-ASC Rating Scale was administered 360 minutes after drug intake. **Results**: Under psilocybin, there were alterations across all dimensions of the 5D-ASC scale, and widespread increases in averaged brain functional connectivity. Further time-varying functional connectivity analysis unveiled a recurrent hyperconnected pattern characterized by low BOLD signal amplitude, suggesting heightened cortical arousal. In terms of neuro-experiential links, canonical correlation analysis showed higher transition probabilities to the hyperconnected pattern with feelings of oceanic boundlessness, and secondly with visionary restructuralization. **Conclusions**: Psilocybin generates profound alterations both at the brain and at the experiential level. We suggest that the brain's tendency to enter a hyperconnected-hyperarousal pattern under psilocybin represents the potential to entertain variant mental associations. These findings illuminate the intricate interplay between brain dynamics and subjective experience under psilocybin, providing insights into the neurophysiology and neuro-experiential qualities of the psychedelic state.

Introduction

Hallucinogens are psychoactive drugs that, historically, have been used to alter conscious experience (1,2). These drugs are divided into the classes of serotonergic psychedelics (e.g., psilocybin), antiglutamatergic dissociatives (e.g., ketamine), anticholinergic deliriants (e.g., scopolamine) and kappa-opioid agonists (e.g., salvinorin A) (3). Research on classical hallucinogens has focused largely on serotonergic psychedelics, such as lysergic acid diethylamide (LSD), ayahuasca, psilocybin, N-dimethyltryptamine (DMT), and mescaline (4). Among them, psilocybin has been one of the most studied psychedelics, possibly due to its potential contribution in treating different disorders (5), such as obsessive-compulsive disorder (6), death-related anxiety (7), depression (8–11), treatment-resistant depression (12–14), major depressive disorder (15), terminal cancer-associated anxiety (11,16), demoralization (17), smoking (18), and alcohol and tobacco addiction (19–21).

The acute phase of psilocybin administration leads to the psychedelic state, which is a specific altered state of consciousness associated with consuming psilocybin and LSD (22). By "state" we here refer to the combination of neurobiological and experiential patterns that are associated with the psychedelic experience (23). In terms of the general experiential alterations, the psychedelic state has been associated with ego dissolution, i.e., the reduction in self-referential awareness, ultimately disrupting self-world boundaries with increasing feelings of unity with others and own surroundings (25,26), unconstrained and hyper-associative cognition (27,28), profound alterations in the perception of time and space (29,30), perceptual alterations, synesthesia, amplification of emotional state (31), and emotional volatility (32). Long-term and enduring effects have also been reported on personality and mood, such as increases in openness and extraversion, decreases in neuroticism, and increases in mindful awareness (33–35). In terms of the neurobiological pattern, the psilocybin administration resulted in increased cerebral connectivity with reduced modularity, whether in the acute or post-acute phase (36–38). Region-wise, there were reports of decreased activity in the thalamus, posterior cingulate cortex, medial prefrontal cortex (10), and altered connectivity of the claustrum (39). Network-wise, decreased connectivity was reported within the default mode network-DMN (1,10), visual network (1), and executive control network (40), as well as reduced segregation of the dorsal attentional network and executive control network (41). These neural counterparts indicate that the subjective effects of psilocybin are linked to alterations in the activity and connectivity of important brain regions involved in information integration and routing when averaged signal analysis is concerned. Dynamic analyses of connectivity patterns after psilocybin administration have shown that the brain tended to recurrently configure into transient

functional patterns with low stability (42). In addition, under psilocybin, there were higher probabilities for the brain to configure into a connectivity pattern characterized by a global cortex-wide positive phase coherence (43). In terms of state transition dynamics, a recent study calculated the minimum network control energy required to transition between states (or maintain the same state) and found that the network control energy landscape was flattened under LSD and psilocybin, meaning that there were more frequent state transitions and increased entropy of brain pattern dynamics (44). Taken together, averaged and dynamic connectivity analyses suggest that psilocybin alters brain function such that the overall neurobiological pattern becomes functionally more connected, more fluid, and less modular.

Of interest is the link between the brain's functional dynamic reconfigurations and the psychedelic state's experiential patterns. A recent investigation correlated the occurrence rates of prominent connectivity patterns (i.e., frontoparietal subsystem and a globally coherent pattern) with subjective drug intensity (SDI) measured on a 10-point Likert scale (43,45). As much as this approach has provided insights into the ensuing psychedelic state, it can be argued that, due to its simplicity, the SDI cannot capture the complexity of the psychedelic state's phenomenological pattern. Here, we adopt a neuro-experiential approach, defined here as the quantification and comparison of both the neurobiological and experiential patterns. This approach allows the investigation of psilocybin's effects on cerebral functional dynamics and, further, the linking of these dynamic spatiotemporal fingerprints with reported experiential alterations measured retrospectively with standardized assessment.

Methods and Materials

This study was conducted according to the code of ethics on human experimentation established by the Declaration of Helsinki (1964) and amended in Fortaleza (Brazil, October 2013). This study was in accordance with the Medical Research Involving Human Subjects Act (WMO) and was approved by the Academic Hospital and the University's Medical Ethics Committee (Maastricht University, Netherlands Trial Register: NTR6505). All participants were fully informed of all procedures, possible adverse reactions, legal rights, responsibilities, expected benefits, and their right to voluntary termination without consequences.

Participants. The present study analyzed previously collected data on 49 healthy participants with previous experience with a psychedelic drug, but not within the past 3 months of the experiment (1). Participants were randomized to receive a single dose of psilocybin (0.17 mg/kg, n=22; 12 male; age=23±2.9 y) or placebo (n=27; 15 male; age=23.1±3.8 y).

Procedure. Participants were familiarized with the test day procedures on a separate training day prior to the treatment conditions. Participants were instructed to refrain from drug use, including psychedelic drugs (≥ 3 months), MDMA/ecstasy (≥ 14 days), alcohol (≥24 hours), and all other drugs of abuse (≥7 days) prior to their testing day. Additionally, participants were asked to refrain from caffeine and nicotine use on the day of the test day. On arrival of a test day, the absence of drug and alcohol use was assessed via a urine drug screen and a breath alcohol screen. An additional pregnancy test was given if participants were female. If all tests were found to be negative, participants were allowed to proceed. After measurements, the treatment was administered orally in a closed cup containing bitter lemon (placebo) or bitter lemon and psilocybin (powder). After 40 minutes, participants were placed in the MRI scanner, where resting state scans and magnetic resonance spectroscopy were performed throughout a 1 hour time window. Six minutes of resting state fMRI were acquired from the participants with eyes open. At the end of the test day (approximately 6 hours after treatment administration), participants were asked to complete measures of retrospective subjective experience (5-Dimensional Altered States of Consciousness (5D-ASC). Participants stayed under supervision until the testing day was complete, and the researcher deemed they were fit to go home.

Phenomenological Assessment. The 5D-ASC Rating Scale is a 94-item self-report scale that assesses the participants' subjective experience after an altered state of consciousness, and as such, is termed a retrospective phenomenological assessment (46,47). In this questionnaire, participants are asked to make a vertical mark on the 10-cm line below each statement to rate the extent to which the following statements applied to their experience: "No, not more than usual" to "Yes, more than usual." The 5D-ASC comprises five dimensions, including *oceanic boundlessness* (OBN), *dread of ego dissolution* (DED), *visionary restructuralization* (VRS), auditory *alterations* (AUA), and *vigilance reduction* (VIR). Further, OBN, DED, and VRS can be decomposed into 11 subscales via a previously published factor analysis (25): OBN: *experience of unity*, *spiritual experience, blissful state*, *insightfulness*, *disembodiment*, DED: *impaired control and cognition*, *anxiety*, and VRS: *complex imagery*, *elementary imagery*, *audio-visual synesthesia*, and *changed meaning of percepts* comprising the 11-ASC scoring scheme.

Analysis encompassed an initial assessment for normality assumptions of the 5D-ASC and its 11-ASC factors using Shapiro-Wilk tests set at α=0.05. In case of violations of normality, non-parametric Mann-Whitney U tests would compare the 5D-ASC and 11-ASC scores between the two groups. P-values were corrected using the Bonferroni method with a significance level set at α=0.05. The effect size was calculated based on Glass rank biserial coefficient (rg).

Neuroimaging Setup. Images were acquired on a 7T Siemens Magnetom scanner (Siemens Medical, Erlangen, Germany) using 32 receiving channel head array Nova coil (NOVA Medical Inc., Wilmington MA). The T1w images were acquired using a magnetization-prepared 2 rapid acquisition gradient-echo (MP2RAGE) sequence collecting 190 sagittal slices following parameters: repetition time (TR) = 4500 ms, echo time (TE) = 2.39 ms, inversion times TI1 /TI2 = 900/2750 ms, flip angle1 = 5°, flip angle2 = 3°, voxel size = 0.9 mm isotropic, bandwidth = 250 Hz/pixel. In addition, 258 whole-brain EPI volumes were acquired at rest (TR = 1400 ms; TE = 21 ms; field of view=198 mm; flip angle = 60°; oblique acquisition orientation; interleaved slice acquisition; 72 slices; slice thickness = 1.5 mm; voxel size = 1.5 × 1.5 × 1.5 mm).

Analysis encompassed:

- Preprocessing**:** fMRI data were preprocessed using a local pipeline based on SPM12 (48) and FSL 6.0.4 (49). After realignment and susceptibility distortion correction (FSL topup (50)), functional data were registered to the high-resolution T1 image, then normalized to the standard MNI space, and finally smoothed using a Gaussian kernel with a full width at half maximum (FWHM) of 6mm. After segmentation of the structural T1 image into grey matter (GM), white matter (WM), and CSF masks, the bias-corrected structural image and all the extracted masks were normalized to the MNI space. Further, WM and CSF masks were eroded by one voxel to remove any overlapping between these tissues and the GM voxels. To denoise functional time series, we used a locally developed pipeline written in Python [nipype package (51)]. In this pipeline, a general linear model (GLM) was fitted to each voxel data separately, regressing out the effect of six movement parameters (translation in x, y, and z directions, and rotation in yaw, roll, and pitch directions) and their first derivative, constant and linear trends using zero-order and first-order Legendre polynomials, 5 principal components of signals in the WM and CSF masks. In addition, outlier detection was performed using the ART toolbox (http://web.mit.edu/swg/software.htm), and outliers were modeled as nuisance regressors in the GLM. Any volume with a movement value of greater than 3 mm, rotation value of greater than 0.05 radians, and z-normalized global signal intensity of greater than 3 was considered an outlier. After regressing out these nuisance regressors, the remaining signal was filtered in the range of [0.008, 0.09] Hz and was used for further analysis. The Schaefer atlas with 100 ROIs and a resolution of 2mm (52) was used to extract the averaged BOLD signals inside each ROI.
- Estimation of Averaged Functional Connectivity. Pearson correlations were calculated between the BOLD time series for every pair of ROIs, subsequently Fisher transformed, resulting in the generation of a 100×100 connectivity matrix for each individual participant. An Independent t-

test was used to compare the 4950 possible between-region connectivity values between the two groups. FDR correction was performed to correct for multiple comparisons. Further, the average of the connectivity values over the whole brain was calculated for each participant and was considered as the overall connectivity value of the brain. An independent t-test was performed to compare the overall connectivity values between psilocybin and placebo groups.

- Estimation of Time-varying Functional Connectivity**.** We used phase-based coherence to extract between-region connectivity patterns at each time point of the scanning session(52,53). For each participant i, after z-normalization of time series at each region r (i.e., $x_{i,r}[t]$), the instantaneous phase of each time series was calculated via Hilbert transform as:

$$\hat{x}_{i,r}(t) = \frac{1}{\pi t} * x_{i,r}(t)$$

where * indicates a convolution operator. Using this transformation, we produced an analytical signal for each regional time series as:

$$x^{a}_{i,r}(t) = x_{i,r}(t) + j\hat{x}_{i,r}(t)$$

where $j = \sqrt{-1}$. From this analytical signal, the instantaneous phase of each time series can be estimated as:

$$\varphi_{i,r}(t) = \tan^{-1}\left(\frac{\hat{x}_{i,r}(t)}{x_{i,r}(t)}\right)$$

After wrapping each instantaneous phase signal of $\varphi_{i,r}(t)$ to the $[-\pi, \pi]$ interval and naming the obtained signal as $\theta_{i,r}(t)$, we calculated a connectivity measure for each pair of regions as the cosine of their phase difference. For example, the connectivity measure between regions r and s in subject i was defined as:

$$conn_{i,r,s}(t) \triangleq \cos\left(\theta_{i,r}(t) - \theta_{i,s}(t)\right)$$

By this definition, completely synchronized time series lead to a connectivity value of 1, completely desynchronized time series produce a connectivity value of zero, and anticorrelated time series produce a connectivity measure of -1. Using this approach, we created a connectivity matrix of 100×100 at each time point t for each subject i that we called $C_i(t)$:

$$C_i(t) \triangleq \left[conn_{i,r,s}(t)\right]_{r,s}$$

After collecting the connectivity matrices across all time points and participants, k-means clustering was applied, with 500 repetitions and 200 iterations at each repetition. With this

technique, four robust and reproducible patterns were extracted as the centroids of the clusters, and each resting connectivity matrix was assigned to one of the extracted patterns. For comprehensive purposes, we performed supplementary analyses by varying the number of clusters k=3- 7.

We calculated the occurrence rate of each pattern defined as the proportion of connectivity matrices assigned to that pattern and was calculated for each subject separately. Independent two-tailed t-tests were used to compare the occurrence rate of each FC pattern between the psychedelic and placebo groups. Bonferroni correction was used to correct the p-values for multiple comparisons across the four connectivity patterns.

- Dynamic state transition modeling**.** To investigate the temporal evolution of the identified connectivity matrices, we defined the extracted patterns as the distinct states of a dynamical system transitioning between them over time using Markov modelling(53). Using this approach, the data of a sample participant could be stated as a sequence of connectivity patterns over time (i.e., $\{P_t \mid t: 1, \dots, T \; and \; P_t \in \{1, \dots, M\}\}$, where M is the number of patterns and T is the number of signal time points). In this case, the probability of transitioning from Pattern I to Pattern J defined as $p(I \rightarrow J)$, considering $I, J \in \{1, .., M\}$, can be calculated as the number of consecutive I, J pairs in the sequence, divided by the total number of transitions from pattern I:

$$p(I \rightarrow J) = \frac{\sum_{t=0}^{T-1}[(P_t == I) \;\&\; (P_{t+1} == J)]}{\sum_{j=1}^{M}\sum_{t=0}^{T-1}[(P_t == I) \;\&\; (P_{t+1} == j)]}$$

This transition probability was estimated for each possible between-state transition and each subject separately. With this approach, we could compare any significant difference in transition probabilities between two groups of subjects. To detect significantly different transition probabilities between the two groups, Wilcoxon rank-sum test was performed on each transition and p-values were FDR-corrected.

- Regional BOLD Amplitude Analysis**.** The Euclidean norm of the BOLD signal was calculated at each ROI as a measure of the power of the signal. Independent t-test was used to compare the regional BOLD signal power between two groups, and p-values were FDR-corrected due to multiple comparisons.
- Neuro-experiential Analysis. A canonical correlation analysis (CCA) was conducted using the sixteen dynamic patterns transition probability variables as features of the neuronal space and the 11-ASC variables as features of the phenomenological space to evaluate the multivariate shared relationship between the two variable sets. CCA is a multivariate latent variable model that identifies associations between two different data modalities (55). Considering matrix $X^{N \times M}$

contains M neuronal features of N subjects, and $Y^{N\times P}$ contains P questionnaire features of N subjects, the objective of the CCA is to find pairs of neuronal and questionnaire weights $w_x^{M\times 1}$ and $w_y^{P\times 1}$ such that the weighted sum of the neuronal and experiential variables maximizes the correlation between the resulting latent variables (canonical variates):

$$\max_{w_x, w_y} corr(Xw_x, Yw_y)$$

After finding latent variables Xw_x and Yw_y that have the maximal correlation, the features in each data modality that have a stronger correlation with their respective latent variable are also significantly associated with one another. To account for over-fitting, we used a permutation test to calculate the significance of correlation values. This was achieved by random shuffling of observations in the neural space compared to the observations in the phenomenological space. The procedure was repeated 100,000 times, and at each iteration, a CCA model was fitted to the data, and the correlation values were calculated. These values were used to construct the null distribution and to calculate the p-value of the observed correlation value in the main analysis. The obtained p-values were FDR-corrected to account for the multiple comparisons.

- Validation of the Results. We analyzed the potential effects of motion, atlas parcellation, and global signal regression on the main results. To quantify motion, we calculated the mean framewise displacement (FD) (56) for each subject as well as for each time-varying connectivity pattern. Independent t-tests were used to compare the mean FD between Placebo and Psilocybin groups as well as between time-varying connectivity patterns. Furthermore, the Pearson correlation between the Mean FD and either mean functional connectivity or mean BOLD signal amplitude was calculated. To investigate the role of sub-cortical regions, we incorporated 19 sub-cortical regions (Brain Stem together with the Thalamus, Caudate, Putamen, Pallidum, Hippocampus, Amygdala, Accumbens area, VentralDC, and Cerebellum in the right and left hemispheres) sourced from the Human Connectome Project (57–59), into the initially utilized Schaefer atlas, resulting in an atlas with 119 regions of interest. Then, we performed both averaged and dynamic functional connectivity analysis using this combined atlas. Finally, to verify the effect of the global signal on the analysis results, we also performed all the analyses after global signal regression (GSR).

Results

Experiential Assessment. All variables of the 5D-ASC and its 11-ASC factors violated the assumption of normality (Table S1). As a result, Mann-Whitney U tests compared the phenomenological outcomes in the two groups. Analyses revealed significant differences in all

dimensions and factors with large effect sizes, such that the psilocybin group had more substantial effects than the placebo (Figure 1A and 1B, Table 1).

Neuroimaging. After psilocybin, whole-brain averaged connectivity increased (independent t-test: t=3.087, p=0.004; Figure 2A). This overall increase was further observed as a cortex-wide increase in the connectivity matrix values (independent t-test on the between-region connectivity values with FDR correction; Figure 2B) and an increase of the averaged connectivity values in the transmodal regions (independent t-test on the regional averaged connectivity values with FDR correction; Figure S1). These alterations in the connectivity values were also accompanied by changes in the BOLD signal amplitude. By calculating the Euclidean norm of the BOLD time series related to each ROI, we found that regional BOLD signal amplitude decreased after psilocybin administration in both posterior and anterior regions compared to the placebo group (independent t-test, FDR-corrected; Figure 2C, and Figure S2). While somatomotor, limbic network, and temporal regions of the DMN did not show significant changes in their signal norm, the highest decrease in BOLD signal amplitude was related to the posterior cingulate cortex and parietal regions of the external control network.

Time-varying analysis revealed variant and distinct patterns of complex inter-areal interactions: one of both correlations and anti-correlations (Pattern 1), one of anti-correlations of the DMN with other networks (Pattern 2), one of global cortex-wide positive connectivity (Pattern 3), and one of low inter-areal connectivity (Pattern 4). Pattern 3 occurred significantly more often in the psilocybin group when compared to the placebo group (independent t-test: t=3.731, p=0.001, $\alpha_{bonferroni}$ = 0.05/4 = 0.0125, Figure 2D). Supplementary analyses using k=3-7 clusters showed that the same connectivity patterns were replicable, and hyperconnectivity had a higher occurrence rate in the psychedelic state (Figure S3). In terms of dynamic transitions, the psilocybin group showed significantly higher transition probabilities towards Pattern 3 from Pattern 1 (Wilcoxon Rank-Sum test: z=2.744, p=0.006), Pattern 3 (z=2.291, p=0.022), and Pattern 4 (z=2.000, p=0.045; Figure 2E). In addition, the psilocybin group showed lower transition probabilities from Pattern 2 to itself compared to the placebo group (z=-2.452, p=0.014).

The neuro-experiential link was investigated with canonical correlation analysis (CCA), by which we estimated the first canonical vector for both the behavioral and neural space that maximized the shared correlation between two spaces (r=0.97, p<0.001). Considering the neural space, the transition probabilities from Pattern 1 to Pattern 3 showed the highest correlation with the first canonical vector of the neural space (r=0.86, p<0.001, Figure 3A). In addition, the transition from Pattern 4 to Pattern 3 (r=0.40, p=0.016) showed a lower significant correlation with the first

canonical vector of the neural space. In the questionnaire space, factors related to oceanic boundlessness (experience of unity: r=0.80, p=0.008, blissful state: r=0.74, p=0.010, insightfulness: r=0.68, p=0.013, spiritual experience: r=0.62, p=0.044) and visionary restructuralization (elementary imagery: r=0.67, p=0.012 and audio-video synesthesia: r=0.61, p=0.021) showed the highest correlations with the first canonical vector of this space (Figure 3B). To account for over-fitting, we used a permutation test to calculate the significance of correlation values. This was achieved by random shuffling of observations in the neural space compared to the observations in the questionnaire space. The procedure was repeated 100,000 times, and at each iteration, a CCA model was fitted to the data, and the correlation values were calculated. These values were used to construct the null distribution and to calculate the p-value of the observed correlation value in the main analysis. The obtained p-values were FDR-corrected to account for the multiple comparisons. To validate the results, we also performed a CCA analysis between the dimensions of the 5D-ASC and the between-state transition probabilities. At the neural space, the transition probability from Pattern 1 to Pattern 3 showed the highest correlation with the first canonical vector of the neural space (r=0.89, p<0.001), and at the questionnaire space, oceanic boundlessness showed the highest correlation with the first canonical vector (r=0.93, p=0.0145; Table 2).

***Validation*.** The analysis of the effect of motion revealed comparable values in terms of mean framewise displacement between the Psilocybin and Placebo group (independent t-test, t=-0.31, p=0.76; Figure S4.A), as well as between the connectivity patterns (Figure S4.B). Additionally, no significant correlations were observed between mean framewise displacement and either mean functional connectivity values (r=0.23, p=0.12) or mean BOLD signal amplitude (r=0.11, p=0.43; Figure S4.C). Furthermore, the connectivity results were replicated even after adding subcortical regions to the parcellation atlas (Figure S5). However, regressing out the global signal led to the absence of a significant increase in functional connectivity values within the psilocybin group (Figures S6.A, and S6.B), as well as the absence of a hyper-connectivity pattern in the dynamic functional analysis (Figure S6.C) as also previously shown (59). Given that the GS amplitude was lower in the Psilocybin group, and that motion values were comparable between the Psilocybin and Placebo groups, we do consider that GS might contain inherent information about the psychedelic state. Therefore, we opted to retain the GS in the main analyses.

Discussion

We investigated the effect of the serotonergic hallucinogen psilocybin on the brain's functional connectome to link it with consciousness alterations to better comprehend how resulting neural and phenomenological changes are interconnected. Overall, we found that psilocybin administration led

to a tendency of the brain to recurrently configure in a globally hyperconnected pattern, which was linked to heightened reports of oceanic boundlessness (experience of unity, blissfulness, insightfulness, and spiritual experience), and visionary restructuralization (complex imagery, elementary imagery, audio-visual synesthesia, and changed meaning of percepts).

Regarding experiential changes, the psilocybin group exhibited significant increases across all dimensions and factors compared to the placebo, including derealization, depersonalization, loss of self-control, visual pseudo-hallucinations (both elementary and complex), audio-visual synesthesia, unity experiences, spiritual insight, bliss, and disembodiment (45), as previously reported (1). These findings demonstrate that a moderate psilocybin dose produces a distinct phenomenological pattern compared to a placebo. Previous research on psilocybin administration also noted measurable changes in various dimensions with dosages ranging from 45 to 315 μg/kg body weight compared to a placebo (60,61). Our data aligns with this dose-dependent phenomenological pattern associated with psilocybin consumption.

Regarding neural changes, the psilocybin group exhibited an overall increase in whole-brain functional connectivity, consistent with previous reports (37). Serotonergic psychedelics, including psilocybin, have been shown to alter the brain's functional organization, promoting greater global integration with increased short-range and long-range functional connections (41,62,63). The dynamic analysis revealed a higher probability of the brain transitioning to a hyperconnected pattern under psilocybin compared to the placebo group, a pattern reported in other psychedelic studies (42). This hyperconnected state, previously shown to be characterized by maximal integration and minimal segregation (53), aligns with the flattened landscape theory, where specific connectivity patterns become less dominant under psychedelics, resulting in increased transition probabilities to the functionally non-specific hyperconnected pattern.[43,63,64]

Additionally, the hyperconnectivity pattern in the psilocybin group was associated with cortex-wide decreases in BOLD signal amplitude. Despite the ongoing debate about global signal (GS) removal in denoising processes due to its reflection of various fMRI nuisance sources, we chose to retain GS in our analysis (66–70). This decision was based on our recent finding that GS can complement extracted connectivity patterns (59). Specifically, we observed that when the hyperconnected pattern coincided with high GS amplitude during wakeful rest, participants were more likely to report instances of mind blanking (59,71). Previously, the GS amplitude served as an indirect measure of general arousal levels, with higher amplitude indicating lower arousal and lower amplitude linked to higher arousal (72–75). After LSD intake, similar results were observed,

showing a decrease in signal variance, which eventually leads to a decrease in GS (76). In our study, the hyperconnectivity pattern was associated with reduced GS amplitude, further contributing to the understanding of the psychedelic state as mediated by high cortical arousal (77). It is important to mention that the hyperconnected pattern was sensitive to GS removal and did not show such signal configuration after the regression (Supplementary Information), which is consistent with our previous work with this method (59).

In neuro-experiential terms, we found a significant association between higher transition probabilities into the hyperconnected pattern and the factors of oceanic boundlessness (OBN) and visionary restructuralization (VRS). OBN entails a positive mood, insight, and unity experiences (25). Previous studies linked positive ego dissolution and oceanic boundlessness to reduced hippocampal glutamate (1) and increased insight to reduced DMN within-network static functional connectivity (27). Our whole-brain dynamic analysis extends this by demonstrating that recurrent hyperconnected states after psilocybin intake can explain unity experiences, characterized by a disruption of the self-world boundary, contrasting with the hyperconnected pattern's atypical minimal segregation profile (53). We propose that unity feelings and visual pseudo-hallucinatory experiences under psilocybin are linked to the brain's inclination for highly integrated patterns, showcasing its capacity for diverse mental associations. This is supported by improved creative thinking dimensions (27,79) attributed to increased between-network functional connectivity of DMN and the frontoparietal network, (28) which resembles the hyperconnected pattern.

Three OBN factors (unity, bliss, insight) had the highest canonical correlations in our analysis, followed by VRS factors. Dimensional-level canonical correlations reinforced OBN's highest association with transition probabilities to the hyperconnected pattern. Despite serotonergic psychedelics being historically labeled as hallucinogens, our findings align with psilocybin studies, emphasizing OBN's primary role in phenomenological outcomes (79–81). OBN's overall importance in the psychedelic state is further supported by research showing that it is linked to increased 5-HT2AR receptor binding potential (60,61), that it predicts functional connectivity changes (82), and that it positively correlates with somatomotor network disconnection (83). Since OBN is defined as the positive valence associated with depersonalization and derealization, it is a key psychometric dimension describing ego phenomenological modifications (25,45). The here performed CCAs on both the 5D-ASC and 11-ASC show OBN and its factors as having the strongest correlations with the latent variable of the neurobiological space. This may suggest OBN as the primary driver of psilocybin's experiential pattern, prompting consideration of more precise terms such as "egotropic" over "hallucinogenic" when discussing its clinical relevance. This is not to

suggest that the other psychometric dimensions/factors do not have importance or clinical relevance. Rather, we mean to raise a discussion around how egotropic effects of psilocybin may be overlooked as reflected in how the drug is labelled or categorized.

Our study has several limitations. First, the absence of concurrent physiological recordings during fMRI scanning restricts tracking arousal levels, leaving us to use GS amplitude as a proxy for cortical arousal. Simultaneous physiological and electrophysiological recordings in future studies could enhance the understanding of neuronal firing during hyperconnected patterns. Second, the between-subject design, which also requires brain anatomy normalization to the MNI space, could hamper the reproducibility of the findings. A proper within-subject design is required in future studies to mitigate this shortcoming. We further recognize that, even with classic mitigations at preprocessing, the effect of motion can still be influencing the obtained findings. Similar effects can also come from the shift in the neurovascular coupling during psychedelics, as recent work in mice with calcium imaging has shown (84). Fourth, we are aware that due to methodological differences using an eyes-open condition during rest our results are not fully in line with other protocols where the psychedelic effects are were maximized with eyes closed. However, as in our past study we showed that the characteristic psychedelic effects could be found in this cohort of subjects even in the eyes open (1), we remain assured that here we also characterize this state adequately. Also, in our past work we identified differences in the DMN which in the present analysis was not straightforward finding. We think that this discrepancy is due to the adoption of a whole-brain network characterization, using an atlas-based parcellation with multiple ROIs, which can reduce the sensitivity of capturing network-level alterations. Lastly, the analysis' reliance on the recruited population may limit generalizability, though previous studies demonstrated replicability and universality of recurrent connectivity patterns in different datasets and brain parcellations (53,59).

In summary, psilocybin induces significant alterations in both brain function and subjective experience, promoting a functionally non-specific hyperconnected organization. The hyperconnected state correlates with reported experiences of oceanic boundlessness and visual pseudo-hallucinations, highlighting the complex interplay between brain dynamics and subjective phenomena potentially reflecting the ability to entertain variant mental associations. In total, these findings illuminate the intricate interplay between brain dynamics and subjective experience under psilocybin and providing insights into the neurophysiology and neuro-experiential qualities of the psychedelic state.

Acknowledgments

Funding: This article was supported by the Belgian Fund for Scientific Research (FRS-FNRS), the European Union's Horizon 2020 Research and Innovation Marie Skłodowska-Curie RISE program NeuronsXnets (grant agreement 101007926), the European Cooperation in Science and Technology COST Action (CA18106), the Léon Fredericq Foundation, and the University and of University Hospital of Liège. The paper appears as preprint on biorxiv https://www.biorxiv.org/content/10.1101/2023.09.18.558309v2. Author contributions: JR & AD contributed to the conception and design of the work; NM acquired the data; SM & LDF contributed with data analysis; all authors contributed to data interpretation; SM, LF, & AD drafted and revised the manuscript; all authors proofread the submitted work. We would like to acknowledge Dr. Camilo Miguel Signorelli for useful discussions during the paper preparation. Data availability: The connectomes and the accompanying covariates used to differentiate individuals can be made available to qualified research institutions upon reasonable request to J.G.R. and a data use agreement executed with Maastricht University. Code availability: All codes used for analysis are freely available at https://gitlab.uliege.be/S.Mortaheb/psychedelics.

Disclosures: The authors report no biomedical financial interests or potential conflicts of interest.

References

1. Mason NL, Kuypers KPC, Müller F, Reckweg J, Tse DHY, Toennes SW, *et al.* (2020): Me, myself, bye: regional alterations in glutamate and the experience of ego dissolution with psilocybin [no. 12]. *Neuropsychopharmacol* 45: 2003–2011.

2. Metzner R (1998): Hallucinogenic Drugs and Plants in Psychotherapy and Shamanism. *Journal of Psychoactive Drugs* 30: 333–341.

3. Volgin AD, Yakovlev OA, Demin KA, Alekseeva PA, Kyzar EJ, Collins C, *et al.* (2019): Understanding Central Nervous System Effects of Deliriant Hallucinogenic Drugs through Experimental Animal Models. *ACS Chem Neurosci* 10: 143–154.

4. Nichols DE (2016): Psychedelics. *Pharmacol Rev* 68: 264–355.

5. Kwan AC, Olson DE, Preller KH, Roth BL (2022): The neural basis of psychedelic action. *Nat Neurosci* 25: 1407–1419.

6. Moreno F, Wiegand C, Taitano K, Delgado P (2006): Safety, Tolerability, and Efficacy of Psilocybin in 9 Patients With Obsessive-Compulsive Disorder. *Journal of Clinical Psychiatry* 67: 1735–1740.

7. Grob CS, Danforth AL, Chopra GS, Hagerty M, McKay CR, Halberstadt AL, Greer GR (2011): Pilot Study of Psilocybin Treatment for Anxiety in Patients With Advanced-Stage Cancer. *Arch Gen Psychiatry* 68: 71.

8. Andersen KAA, Carhart-Harris R, Nutt DJ, Erritzoe D (2021): Therapeutic effects of classic serotonergic psychedelics: A systematic review of modern-era clinical studies. *Acta Psychiatr Scand* 143: 101–118.

9. Carhart-Harris RL, Giribaldi B, Watts R, Baker-Jones M, Murphy-Beiner A, Murphy R, *et al.* (2021): Trial of Psilocybin versus Escitalopram for Depression. *N Engl J Med* 384: 1402–1411.

10. Carhart-Harris RL, Erritzoe D, Williams T, Stone JM, Reed LJ, Colasanti A, *et al.* (2012): Neural correlates of the psychedelic state as determined by fMRI studies with psilocybin. *Proc Natl Acad Sci USA* 109: 2138–2143.

11. Ross S, Bossis A, Guss J, Agin-Liebes G, Malone T, Cohen B, *et al.* (2016): Rapid and sustained symptom reduction following psilocybin treatment for anxiety and depression in patients with life-threatening cancer: a randomized controlled trial. *J Psychopharmacol* 30: 1165–1180.

12. Carhart-Harris RL, Bolstridge M, Rucker J, Day CMJ, Erritzoe D, Kaelen M, *et al.* (2016): Psilocybin with psychological support for treatment-resistant depression: an open-label feasibility study. *The Lancet Psychiatry* 3: 619–627.

13. Carhart-Harris RL, Roseman L, Bolstridge M, Demetriou L, Pannekoek JN, Wall MB, *et al.* (2017): Psilocybin for treatment-resistant depression: fMRI-measured brain mechanisms. *Sci Rep* 7: 13187.

14. Carhart-Harris RL, Bolstridge M, Day CMJ, Rucker J, Watts R, Erritzoe DE, *et al.* (2018): Psilocybin with psychological support for treatment-resistant depression: six-month follow-up. *Psychopharmacology* 235: 399–408.

15. Davis AK, Barrett FS, May DG, Cosimano MP, Sepeda ND, Johnson MW, *et al.* (2021): Effects of Psilocybin-Assisted Therapy on Major Depressive Disorder: A Randomized Clinical Trial. *JAMA Psychiatry* 78: 481.

16. Griffiths RR, Johnson MW, Carducci MA, Umbricht A, Richards WA, Richards BD, *et al.* (2016): Psilocybin produces substantial and sustained decreases in depression and anxiety in patients with life-threatening cancer: A randomized double-blind trial. *J Psychopharmacol* 30: 1181–1197.

17. Anderson BT, Danforth A, Daroff PR, Stauffer C, Ekman E, Agin-Liebes G, *et al.* (2020): Psilocybin-assisted group therapy for demoralized older long-term AIDS survivor men: An open-label safety and feasibility pilot study. *EClinicalMedicine* 27: 100538.

18. Johnson MW, Garcia-Romeu A, Griffiths RR (2017): Long-term follow-up of psilocybin-facilitated smoking cessation. *The American Journal of Drug and Alcohol Abuse* 43: 55–60.

19. Bogenschutz MP, Forcehimes AA, Pommy JA, Wilcox CE, Barbosa P, Strassman RJ (2015): Psilocybin-assisted treatment for alcohol dependence: A proof-of-concept study. *J Psychopharmacol* 29: 289–299.

20. Garcia-Romeu A, Davis AK, Erowid F, Erowid E, Griffiths RR, Johnson MW (2019): Cessation and reduction in alcohol consumption and misuse after psychedelic use. *J Psychopharmacol* 33: 1088–1101.

21. Johnson MW, Garcia-Romeu A, Cosimano MP, Griffiths RR (2014): Pilot study of the 5-HT $_{2A}$ R agonist psilocybin in the treatment of tobacco addiction. *J Psychopharmacol* 28: 983–992.

22. Bayne T, Carter O (2018): Dimensions of consciousness and the psychedelic state. *Neuroscience of Consciousness* 2018: niy008.

23. Rock A, Krippner S (2007): Does the Concept of "Altered States of Consciousness" Rest on a Mistake? *International Journal of Transpersonal Studies* 26. https://doi.org/10.24972/ijts.2007.26.1.33

24. Nour MM, Carhart-Harris RL (2017): Psychedelics and the science of self-experience. *Br J Psychiatry* 210: 177–179.

25. Studerus E, Gamma A, Vollenweider FX (2010): Psychometric Evaluation of the Altered States of Consciousness Rating Scale (OAV) ((V. Bell, editor)). *PLoS ONE* 5: e12412.

26. Girn M, Mills C, Roseman L, Carhart-Harris RL, Christoff K (2020): Updating the dynamic framework of thought: Creativity and psychedelics. *NeuroImage* 213: 116726.

27. Mason NL, Kuypers KPC, Reckweg JT, Müller F, Tse DHY, Da Rios B, *et al.* (2021): Spontaneous and deliberate creative cognition during and after psilocybin exposure. *Transl Psychiatry* 11: 209.

28. Carhart-Harris RL, Leech R, Hellyer PJ, Shanahan M, Feilding A, Tagliazucchi E, *et al.* (2014): The entropic brain: a theory of conscious states informed by neuroimaging research with psychedelic drugs. *Front Hum Neurosci* 8. https://doi.org/10.3389/fnhum.2014.00020

29. Griffiths RR, Richards WA, McCann U, Jesse R (2006): Psilocybin can occasion mystical-type experiences having substantial and sustained personal meaning and spiritual significance. *Psychopharmacology* 187: 268–283.

30. Preller KH, Vollenweider FX (2018): Phenomenology, Structure, and Dynamic of Psychedelic States. In: Halberstadt AL, Vollenweider FX, Nichols DE, editors. *Behavioral Neurobiology of Psychedelic Drugs*. Berlin, Heidelberg: Springer, pp 221–256.

31. Majić T, Schmidt TT, Gallinat J (2015): Peak experiences and the afterglow phenomenon: When and how do therapeutic effects of hallucinogens depend on psychedelic experiences? *J Psychopharmacol* 29: 241–253.

32. Erritzoe D, Roseman L, Nour MM, MacLean K, Kaelen M, Nutt DJ, Carhart-Harris RL (2018): Effects of psilocybin therapy on personality structure. *Acta Psychiatr Scand* 138: 368–378.

33. MacLean KA, Johnson MW, Griffiths RR (2011): Mystical experiences occasioned by the hallucinogen psilocybin lead to increases in the personality domain of openness. *J Psychopharmacol* 25: 1453–1461.

34. Madsen MK, Fisher PM, Stenbæk DS, Kristiansen S, Burmester D, Lehel S, *et al.* (2020): A single psilocybin dose is associated with long-term increased mindfulness, preceded by a proportional change in neocortical 5-HT2A receptor binding. *European Neuropsychopharmacology* 33: 71–80.

35. Daws RE, Timmermann C, Giribaldi B, Sexton JD, Wall MB, Erritzoe D, *et al.* (2022): Increased global integration in the brain after psilocybin therapy for depression. *Nat Med* 28: 844–851.

36. Preller KH, Duerler P, Burt JB, Ji JL, Adkinson B, Stämpfli P, *et al.* (2020): Psilocybin Induces Time-Dependent Changes in Global Functional Connectivity. *Biological Psychiatry* 88: 197–207.

37. Roseman L, Leech R, Feilding A, Nutt DJ, Carhart-Harris RL (2014): The effects of psilocybin and MDMA on between-network resting state functional connectivity in healthy volunteers. *Front Hum Neurosci* 8. https://doi.org/10.3389/fnhum.2014.00204

38. Barrett FS, Krimmel SR, Griffiths RR, Seminowicz DA, Mathur BN (2020): Psilocybin acutely alters the functional connectivity of the claustrum with brain networks that support perception, memory, and attention. *NeuroImage* 218: 116980.

39. McCulloch DE-W, Madsen MK, Stenb DS (2022): Lasting effects of a single psilocybin dose on resting-state functional connectivity in healthy individuals. *Journal of Psychopharmacology* 11.

40. Madsen MK, Stenbæk DS, Arvidsson A, Armand S, Marstrand-Joergensen MR, Johansen SS, *et al.* (2021): Psilocybin-induced changes in brain network integrity and segregation correlate with

plasma psilocin level and psychedelic experience. *European Neuropsychopharmacology* 50: 121–132.

41. Petri G, Expert P, Turkheimer F, Carhart-Harris R, Nutt D, Hellyer PJ, Vaccarino F (2014): Homological scaffolds of brain functional networks. *J R Soc Interface* 11: 20140873.

42. Lord L-D, Expert P, Atasoy S, Roseman L, Rapuano K, Lambiotte R, *et al.* (2019): Dynamical exploration of the repertoire of brain networks at rest is modulated by psilocybin. *NeuroImage* 199: 127–142.

43. Singleton SP, Luppi AI, Carhart-Harris RL, Cruzat J, Roseman L, Nutt DJ, *et al.* (2022): Receptor-informed network control theory links LSD and psilocybin to a flattening of the brain's control energy landscape. *Nat Commun* 13: 5812.

44. Olsen AS, Lykkebo-Valløe A, Ozenne B, Madsen MK, Stenbæk DS, Armand S, *et al.* (2022): Psilocybin modulation of time-varying functional connectivity is associated with plasma psilocin and subjective effects. *NeuroImage* 264: 119716.

45. Dittrich A (1998): The standardized psychometric assessment of altered states of consciousness (ASCs) in humans. *Pharmacopsychiatry* 31: 80–84.

46. Pekala RJ (2013): *Quantifying Consciousness: An Empirical Approach*. Springer Science & Business Media.

47. Penny WD, Friston KJ, Ashburner JT, Kiebel SJ, Nichols TE (2011): *Statistical Parametric Mapping: The Analysis of Functional Brain Images*. Elsevier.

48. Jenkinson M, Beckmann CF, Behrens TEJ, Woolrich MW, Smith SM (2012): FSL. *NeuroImage* 62: 782–790.

49. Andersson JLR, Skare S, Ashburner J (2003): How to correct susceptibility distortions in spin-echo echo-planar images: application to diffusion tensor imaging. *NeuroImage* 20: 870–888.

50. Gorgolewski K, Burns CD, Madison C, Clark D, Halchenko YO, Waskom ML, Ghosh SS (2011): Nipype: A Flexible, Lightweight and Extensible Neuroimaging Data Processing Framework in Python. *Front Neuroinform* 5. https://doi.org/10.3389/fninf.2011.00013

51. Schaefer A, Kong R, Gordon EM, Laumann TO, Zuo X-N, Holmes AJ, *et al.* (2018): Local-Global Parcellation of the Human Cerebral Cortex from Intrinsic Functional Connectivity MRI. *Cerebral Cortex* 28: 3095–3114.

52. Barttfeld P, Uhrig L, Sitt JD, Sigman M, Jarraya B, Dehaene S (2015): Signature of consciousness in the dynamics of resting-state brain activity. *Proc Natl Acad Sci USA* 112: 887–892.

53. Demertzi A, Tagliazucchi E, Dehaene S, Deco G, Barttfeld P, Raimondo F, *et al.* (2019): Human consciousness is supported by dynamic complex patterns of brain signal coordination. *Science Advances* 5: eaat7603.

54. Mihalik A, Chapman J, Adams RA, Winter NR, Ferreira FS, Shawe-Taylor J, Mourão-Miranda J (2022): Canonical Correlation Analysis and Partial Least Squares for Identifying Brain–Behavior Associations: A Tutorial and a Comparative Study. *Biological Psychiatry: Cognitive Neuroscience and Neuroimaging* 7: 1055–1067.

55. Power JD, Mitra A, Laumann TO, Snyder AZ, Schlaggar BL, Petersen SE (2014): Methods to detect, characterize, and remove motion artifact in resting state fMRI. *NeuroImage* 84: 320–341.

56. Griffa A, Amico E, Liégeois R, Van De Ville D, Preti MG (2022): Brain structure-function coupling provides signatures for task decoding and individual fingerprinting. *NeuroImage* 250: 118970.

57. Glasser MF, Sotiropoulos SN, Wilson JA, Coalson TS, Fischl B, Andersson JL, *et al.* (2013): The minimal preprocessing pipelines for the Human Connectome Project. *NeuroImage* 80: 105–124.

58. Fischl B, Salat DH, Busa E, Albert M, Dieterich M, Haselgrove C, *et al.* (2002): Whole Brain Segmentation. *Neuron* 33: 341–355.

59. Mortaheb S, Van Calster L, Raimondo F, Klados MA, Boulakis PA, Georgoula K, *et al.* (2022): Mind blanking is a distinct mental state linked to a recurrent brain profile of globally positive connectivity during ongoing mentation. *Proceedings of the National Academy of Sciences* 119: e2200511119.

599 60. Hasler F, Grimberg U, Benz MA, Huber T, Vollenweider FX (2004): Acute psychological and
600 physiological effects of psilocybin in healthy humans: a double-blind, placebo-controlled
601 dose?effect study. *Psychopharmacology* 172: 145–156.
602 61. Quednow BB, Kometer M, Geyer MA, Vollenweider FX (2012): Psilocybin-Induced Deficits in
603 Automatic and Controlled Inhibition are Attenuated by Ketanserin in Healthy Human Volunteers
604 [no. 3]. *Neuropsychopharmacol* 37: 630–640.
605 62. Tagliazucchi E, Roseman L, Kaelen M, Orban C, Muthukumaraswamy SD, Murphy K, *et al.* (2016):
606 Increased Global Functional Connectivity Correlates with LSD-Induced Ego Dissolution. *Current*
607 *Biology* 26: 1043–1050.
608 63. Timmermann C, Roseman L, Haridas S, Rosas FE, Luan L, Kettner H, *et al.* (2023): Human brain effects
609 of DMT assessed via EEG-fMRI. *Proc Natl Acad Sci USA* 120: e2218949120.
610 64. Singleton SP, Luppi AI, Carhart-Harris RL, Cruzat J, Roseman L, Nutt DJ, *et al.* (2022): Receptor-
611 informed network control theory links LSD and psilocybin to a flattening of the brain's control
612 energy landscape [no. 1]. *Nat Commun* 13: 5812.
613 65. Carhart-Harris RL, Friston KJ (2019): REBUS and the Anarchic Brain: Toward a Unified Model of the
614 Brain Action of Psychedelics ((E. L. Barker, editor)). *Pharmacol Rev* 71: 316–344.
615 66. Murphy K, Fox MD (2017): Towards a consensus regarding global signal regression for resting state
616 functional connectivity MRI. *NeuroImage* 154: 169–173.
617 67. Power JD, Plitt M, Laumann TO, Martin A (2017): Sources and implications of whole-brain fMRI signals
618 in humans. *NeuroImage* 146: 609–625.
619 68. Chang C, Glover GH (2010): Time–frequency dynamics of resting-state brain connectivity measured
620 with fMRI. *NeuroImage* 50: 81–98.
621 69. Zhu DC, Tarumi T, Khan MA, Zhang R (2015): Vascular Coupling in Resting-State FMRI: Evidence from
622 Multiple Modalities. *J Cereb Blood Flow Metab* 35: 1910–1920.

623 70. Colenbier N, Van de Steen F, Uddin LQ, Poldrack RA, Calhoun VD, Marinazzo D (2020): Disambiguating
624 the role of blood flow and global signal with partial information decomposition. *NeuroImage* 213:
625 116699.
626 71. Ward AF, Wegner DM (2013): Mind-blanking: when the mind goes away. *Front Psychol* 4.
627 https://doi.org/10.3389/fpsyg.2013.00650
628 72. Fukunaga M, Horovitz SG, Van Gelderen P, De Zwart JA, Jansma JM, Ikonomidou VN, *et al.* (2006):
629 Large-amplitude, spatially correlated fluctuations in BOLD fMRI signals during extended rest and
630 early sleep stages. *Magnetic Resonance Imaging* 24: 979–992.
631 73. Nilsonne G, Tamm S, Schwarz J, Almeida R, Fischer H, Kecklund G, *et al.* (2017): Intrinsic brain
632 connectivity after partial sleep deprivation in young and older adults: results from the Stockholm
633 Sleepy Brain study. *Sci Rep* 7: 9422.
634 74. Wong CW, Olafsson V, Tal O, Liu TT (2013): The amplitude of the resting-state fMRI global signal is
635 related to EEG vigilance measures. *NeuroImage* 83: 983–990.
636 75. Liu X, de Zwart JA, Schölvinck ML, Chang C, Ye FQ, Leopold DA, Duyn JH (2018): Subcortical evidence
637 for a contribution of arousal to fMRI studies of brain activity. *Nat Commun* 9: 395.
638 76. Carhart-Harris RL, Muthukumaraswamy S, Roseman L, Kaelen M, Droog W, Murphy K, *et al.* (2016):
639 Neural correlates of the LSD experience revealed by multimodal neuroimaging. *Proc Natl Acad Sci*
640 *U S A* 113: 4853–4858.
641 77. Carhart-Harris RL, Leech R, Erritzoe D, Williams TM, Stone JM, Evans J, *et al.* (2013): Functional
642 Connectivity Measures After Psilocybin Inform a Novel Hypothesis of Early Psychosis.
643 *Schizophrenia Bulletin* 39: 1343–1351.
644 78. Mason NL, Kuypers KPC, Reckweg JT, Müller F, Tse DHY, Da Rios B, *et al.* (2021): Spontaneous and
645 deliberate creative cognition during and after psilocybin exposure [no. 1]. *Transl Psychiatry* 11: 1–
646 13.
647 79. Nichols DE (2016): Psychedelics ((E. L. Barker, editor)). *Pharmacol Rev* 68: 264–355.

80. Metzner R (2005): Psychedelic, Psychoactive, and Addictive Drugs and States of Consciousness. *Mind-Altering Drugs : The Science of Subjective Experience*. Oxford ; New York : Oxford University Press. Retrieved August 30, 2023, from http://archive.org/details/mindalteringdrug0000unse

81. Rotz R von, Schindowski EM, Jungwirth J, Schuldt A, Rieser NM, Zahoranszky K, *et al.* (2023): Single-dose psilocybin-assisted therapy in major depressive disorder: a placebo-controlled, double-blind, randomised clinical trial. *eClinicalMedicine* 56. https://doi.org/10.1016/j.eclinm.2022.101809

82. Smigielski L, Scheidegger M, Kometer M, Vollenweider FX (2019): Psilocybin-assisted mindfulness training modulates self-consciousness and brain default mode network connectivity with lasting effects. *NeuroImage* 196: 207–215.

83. Preller KH, Burt JB, Ji JL, Schleifer CH, Adkinson BD, Stämpfli P, *et al.* (2018): Changes in global and thalamic brain connectivity in LSD-induced altered states of consciousness are attributable to the 5-HT2A receptor. *eLife* 7: e35082.

84. Padawer-Curry JA, Snyder AZ, Bice AR, Wang X, Nicol GE, McCall JG, *et al.* (2023, September 24): Psychedelic 5-HT2A receptor agonism: neuronal signatures and altered neurovascular coupling. bioRxiv, p 2023.09.23.559145.

Figure 1. Substantial alterations in subjective experience were reported after psilocybin administration compared to placebo. A) The assessment of five dimensions of altered states of consciousness questionnaire (5D-ASC) showed that the administration of psilocybin significantly altered subjective experience in all dimensions. **B)** The same effect can also be observed considering the 11 factors of altered states of consciousness (11-ASC). Notes, OBN: Oceanic Boundlessness, DED: Dread of Ego Dissolution, VRS: Visionary Restructuralization. Radar plots illustrate group means for each dimension/factor.

Figure 2. After psilocybin administration, there was an overall cerebral tendency to show more re-occurrence of a functional hyper-connectivity pattern. A) Averaged functional connectivity expressed as Fisher-transformed correlation values increased significantly after psilocybin administration compared to the placebo group. **B)** There were higher inter-regional connectivity values in the psilocybin group. The matrix represents t-values comparing the connectivity matrices of the psilocybin group and those of the placebo group (contrast: psilocybin minus placebo). Only significant difference values are colored. **C)** The BOLD amplitude of posterior and anterior brain regions decreased after psilocybin administration, while the amplitude of somatomotor and limbic areas, as well as the temporal regions of default more network (DMN), remain unchanged. Colors are based on t-values comparing the Euclidean norm of BOLD time series in the psilocybin group and the placebo group at each ROI; only significant difference values are colored. **D)** The functional connectome reconfigures in four connectivity patterns, ranging from complex inter-areal interactions (Pattern 1) to a low inter-areal connectivity profile (Pattern 4). After psilocybin administration, there was a significant increase in the occurrence rate of the global cortex-wide positive connectivity (Pattern 3). The connectivity matrices are colored based on the connectivity value: from dark blue to dark red corresponds to connectivity values from -1 to +1. Violin plots represent the distribution of patterns' occurrence rates across participants. **E)** The transition probability from other patterns to Pattern 3 increased in the psilocybin group. Arrows indicate transitions between functional connectivity states. Green corresponds to significantly higher transition probabilities (Wilcoxon Rank-Sum test) for the psilocybin group compared to the placebo, and red corresponds to significantly higher transition probabilities for the placebo compared to the psilocybin group.

Figure 3. **The neuro-experiential analysis indicated that transitions to the hyperconnected Pattern 3 were linked to the factors of oceanic boundlessness and visionary restructuralization. A)** In the neural space, the canonical correlation analysis showed that the

transition probabilities to the hyperconnected pattern had the highest correlation with the first canonical vector of the space. *Notes*: Demonstrated p-values are related to the significant correlation values and are FDR-corrected. The x-axis represents pattern transitions, e.g. T13: transition from Pattern 1 to Patten 3. **B)** In the phenomenological space, factors related to the dimension of oceanic boundlessness and visionary restructuralization showed the highest correlation with the first canonical vector of the space. Bars represent correlation values of each factor to the first canonical vector of its associated space. *Notes:* OBN: oceanic boundlessness, VRS: visionary restructuralization, DED: dread of ego dissolution, Unity: experience of unity, Bliss: blissful state, Insight: insightfulness, Spirit: spiritual experience, Disembody: disembodiment, ElemImg: elementary imagery, Synesth: audio-visual synesthesia, CmpxImg: complex imagery, ChangeMean: changed meaning of percept, Impair: Impaired control and cognition, AUA: auditory alterations, VIR: vigilance reduction.

Table 1. There were substantial changes in subjective experience after psilocybin administration compared to placebo. Mann-Whitney U test results of comparison between 11-ASC factors of the Psilocybin and Placebo groups. rg = Glass rank biserial coefficient effect size.

Table 2. The neuro-experiential analysis indicated that transitions from Pattern 1 to the hyperconnected Pattern 3 were linked to Oceanic Boundlessness. Canonical correlation analysis between between-state transition probabilities and five dimensions of the 5D-ASC. The results are sorted from the highest correlation to the lowest.

Table 1

		Psilocybin (n=21)		Placebo (n=26)		Stats (MW-U test)		
		mean	**SD**	**mean**	**SD**	**U**	**rg**	**p**
5D-ASC	Oceanic Boundlessness	35.09	23.58	3.78	5.56	528.5	.936	**< 0.001**
	Dread of Ego Dissolution	20.54	17.12	3.94	8.05	494	.81	**< 0.001**
	Visionary Restructuralization	42.97	19.20	5.33	9.23	528.5	.936	**< 0.01**
	Auditory Alterations	16.99	17.18	4.69	12.97	458.5	.679	**< 0.001**
	Vigilance Reduction	28.18	20.43	13.99	16.33	400.5	.467	**< 0.001**
11-ASC	Insightfulness	42.44	29.77	4.99	7.39	508	0.861	**<0.001**
	Spiritual Experience	21.73	22.04	3.33	6.91	435	0.593	**<0.001**
	Experience of Unity	33.27	30.57	2.85	4.70	483.5	0.771	**<0.001**
	Blissful State	35.65	27.02	4.36	7.04	489	0.791	**<0.001**
	Disembodiment	20.65	25.71	1.74	1.82	434	0.59	**<0.001**
	Anxiety	19.55	22.57	3.01	4.30	430	0.575	**<0.001**
	Impaired Control and Cognition	24.29	18.35	4.77	12.51	497	0.821	**<0.001**
	Changed Meaning of Percept	36.75	29.65	4.24	8.92	495.5	0.815	**<0.001**
	Audio-Visual Synesthesia	49.54	22.82	4.94	12.99	525	0.923	**<0.001**
	Complex Imagery	36.43	25.49	6.22	12.03	528.5	0.839	**<0.001**
	Elementary Imagery	49.25	21.95	5.68	9.24	502	0.943	**<0.001**

Table 2.

	Factor	Correlation Coefficient	p-value	p-value (FDR-Corrected)
Neural Space	T13	0.89	1.00e-05	1.60e-04 ***
	T23	0.44	3.07e-02	1.64e-01
	T43	0.43	1.71e-03	1.37e-02 *
	T33	0.25	5.94e-02	1.91e-01
	T21	0.23	4.86e-02	1.91e-01
	T14	0.12	1.58e-01	4.22e-01
	T32	0.09	2.90e-01	5.80e-01
	T24	0.09	2.51e-01	5.73e-01
	T31	-0.01	5.37e-01	9.55e-01
	T44	-0.08	7.61e-01	9.92e-01
	T11	-0.09	6.61e-01	9.92e-01
	T41	-0.17	8.38e-01	9.92e-01
	T34	-0.27	9.70e-01	9.92e-01
	T22	-0.33	9.69e-01	9.92e-01
	T12	-0.34	9.84e-01	9.92e-01
	T42	-0.34	9.92e-02	9.92e-01
Phenomenological Space	OBN	0.93	2.90e-03	1.45e-02 *
	VRS	0.74	4.29e-02	1.07e-01
	DED	0.46	2.02e-01	3.32e-01
	AUA	0.35	2.66e-01	3.32e-01
	VIR	0.11	4.54e-01	4.54e-01

Tij: probability of transition from Pattern i to Pattern j. OBN: oceanic boundlessness, VRS: visionary restructuralization, DED: dread of ego dissolution, AUA: auditory alteration, VIR: vigilance reduction.